KLL dielectronic-recombination measurement for Li-like to O-like gold

Gang Xiong,[1] Jiyan Zhang,[1] Zhimin Hu,[1,*] Nobuyuki Nakamura,[2] Yueming Li,[3] Xiaoying Han,[3] Jiamin Yang,[1] and Baohan Zhang[1]

[1]*Research Center of Laser Fusion, China Academy of Engineering Physics, P. O. Box 919-986, Mianyang 621900, China*

[2]*Institute for Laser Science, The University of Electro-Communications, Chofu, Tokyo 182-8585, Japan*

[3]*Institute of Applied Physics and Computational Mathematics, P. O. Box 8009, Beijing 100088, China*

(Received 1 September 2013; published 10 October 2013)

We report the experimentally determined *KLL* dielectronic-recombination (DR) resonance strengths of Li- to O-like gold. The measurement was performed with an electron beam ion trap, and the x rays emitted from DR and radiative recombination (RR) were both observed. The DR resonance strengths were determined by normalizing DR x-ray intensities to the theoretical RR cross sections. The experimental DR resonance strengths are compared with the theoretical ones, and the comparison shows a good agreement. The scaling laws of the *KLL* DR resonance strengths were obtained as a function of atomic number for B-like and C-like ions by fitting the present and existing experimental results.

DOI: 10.1103/PhysRevA.88.042704 PACS number(s): 34.80.Lx, 52.20.Fs, 31.15.V−

I. INTRODUCTION

Dielectronic recombination (DR), known as a resonant capture process, plays an important role in determining the charge state distribution of hot plasmas [1–4]. *KLL* DR corresponds to a process in which a free electron is captured into an L shell and a K-shell electron is excited into an L shell simultaneously. However, radiative recombination (RR) is the direct electron-ion combination accompanied with photon emissions.

DR studies on highly charged ions are of importance for testing the relativistic effects. For few-electron heavy ions, the Breit interaction effect brings about significant enhancement for the DR resonance strength [5,6]. The strong quantum interference effect between DR and RR is expected as their amplitudes become comparable [7,8]. To date, numerous investigations have been carried out for measuring DR resonance strengths of highly charged ions. Some measurements focused on H-like [9–14] and He-like ions [15–23]. However, there are few experimental studies on DR resonance strengths of open-shelled lower-charged ions [24–26].

In this paper, we report an experiment for measuring DR resonance strengths of Li- to O-like gold. Gold was chosen not only for its large atomic number, but also for its importance in the inertial confinement fusion research field where gold is the primary candidate of laser to x-ray conversion material [27,28]. The experimental DR resonance strengths were obtained by a fit procedure in which the DR x-ray intensities were normalized to the theoretical RR cross sections. In order to analyze the experiment, the theoretical DR and RR cross sections were calculated using flexible atomic code (FAC) [29,30].

II. EXPERIMENT

The present experiment was performed at the Tokyo electron beam ion trap (Tokyo-EBIT) [31,32]. Figure 1 shows the schematic arrangement for the experiment. The electron beam energy was scanned by applying a sawtooth waveform potential to the trapping region with a rate of 2.4 V/μs between 40 to 52 kV, where the gold *KLL* DR resonances of the interested charge states were expected to take place. The electron beam was compressed by an axial magnetic field of 4 T in the trap region and the beam current was fixed at 50 mA. The neutral gold atoms were introduced into the trapping region through an effusion cell [33], then successively ionized and excited by the energetic electron beam. A high-purity germanium detector mounted perpendicularly to the electron beam was used to observe the x rays emitted from the excited gold ions in the trapping region. When an x ray was detected, the electron beam energy was recorded simultaneously.

A typical two-dimensional histogram of the electron-ion recombination processes observed in the *KLL* region is shown in Fig. 2. The x-ray energy was calibrated using the radiation from radio isotopes, whereas the electron energy was calibrated to the theoretical DR resonant energies. The two clearly separated diagonal bands represent RR x-ray emission into $n = 2$ shells. The upper and lower bands correspond to the total angular momentum $J = \frac{1}{2}$ and $\frac{3}{2}$, respectively. Along the two RR bands, several distinct groups that appear clearly at different electron energies indicate the DR resonances. The DR resonances at the lower-, middle-, and higher-electron energies are referred to as $KL_{12}L_{12}$, $KL_{12}L_3$, and KL_3L_3, respectively. Here, L_{12} denotes the $2s_{1/2}$ and $2p_{1/2}$ levels and L_3 the $2p_{3/2}$ level. $KL_{12}L_3$ indicates that the excitation and capture of electrons into $J = \frac{1}{2}$ and $\frac{3}{2}$ levels. $KL_{12}L_{12}$ and KL_3L_3 can be explained in a similar way. The DR resonances at the lower and higher x-ray energies correspond to the radiative decays of $2p_{1/2} \rightarrow 1s$ and $2p_{3/2} \rightarrow 1s$, respectively. A more detailed analysis of the experimental DR resonance strengths is presented in Sec. IV.

III. THEORETICAL CALCULATIONS

The resonant strength for an isolated DR resonance from a state i via a doubly excited state d to a final state f can be expressed as

$$S_{idf} = \int_0^\infty \sigma_{idf}(E)dE = \frac{g_d}{2g_i}\frac{\pi^2\hbar^3 A^a_{di}}{m_e E_{\rm res}}\frac{A^r_{df}}{\sum A^r + \sum A^a}, \quad (1)$$

*Corresponding author: zhimin.hu@yahoo.com

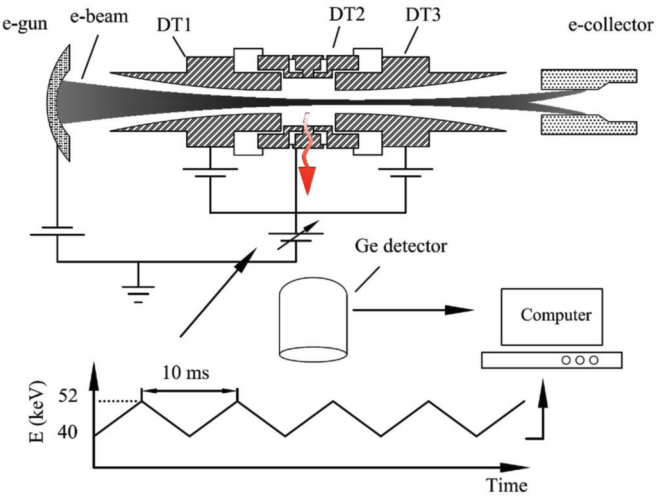

FIG. 1. (Color online) Schematic of the experimental arrangement for x-ray measurements of dielectronic recombination of highly charged gold ions.

where $\sigma_{idf}(E)$ is the DR cross section, $E_{\rm res}$ the resonant energy, $\hbar$ the Dirac constant, m_e the electron mass, g_d and g_i the statistical weights of the states d and i, respectively. A^r_{df} is the Einstein coefficient for spontaneous emission from state d to f, and A^a_{di} the coefficient for autoionization from state d to i. The summation is over all the possible autoionization and radiative decay channels from the doubly excited states.

FAC was used to calculate all of the atomic data, including energy levels, radiative transition rates, and autoionization rates. FAC is a relativistic configuration interaction program developed by Gu [29,30] and has been extensively used for DR theoretical calculations [34–39]. The present theoretical results were obtained with fully relativistic treatment including the Breit interaction, as listed in Tables I to VI.

Owing to the fact that the x rays were observed at 90° with respect to the electron beam propagation direction in the present experiment, the anisotropic angular distribution of the DR x-ray emissions must be taken into account. Therefore, the differential resonance strength observed in the present experiment is written as

$$\frac{dS_{idf}}{d\Omega} = \frac{S_{idf}}{4\pi} W_{d\to f}(90^\circ), \tag{2}$$

where $W_{d\to f}(90^\circ)$ is the angular distribution correction coefficient at 90°, which has been described in detail in our previous papers [13,40].

Conversely, it is also possible to deduce the total resonance strength from the experimental differential resonance strength using the expression,

$$S = \frac{4\pi}{W^*}\frac{dS}{d\Omega}, \tag{3}$$

where W^* is the effective angular correction coefficient, and defined as

$$W^* = \frac{\sum_{i,d,f} W_{d\to f}(90^\circ) S_{idf}}{\sum_{i,d,f} S_{idf}}. \tag{4}$$

Due to the natural width of the doubly excited states, DR resonances have a Lorentzian profile, which is expressed as

$$L(E) = \frac{2}{\pi\Gamma}\frac{1}{1+\epsilon^2}, \tag{5}$$

where $\epsilon = 2(E - E_{\rm res})/\Gamma$, Γ is the natural width of the doubly excited states. In the case of the strong interference with the direct radiative recombination, the asymmetric Fano profile is generally used, which is expressed as

$$F(E) = \frac{2}{q^2\pi\Gamma}\left[\frac{(q+\epsilon)^2}{1+\epsilon^2} - 1\right], \tag{6}$$

where q is the Fano factor. It is noted that $F(E)$ is equivalent to $L(E)$ when $q \to \infty$. The Fano profile has been used to describe the interference effects between DR and RR in highly charged heavy ions [7,8]. The $KL_{12}L_3$ resonance often shows a clear asymmetric profile for some particular charge states [41]. However, the asymmetric profile was not significant in Fig. 3 since it was obtained by projecting all of the x-ray counts onto the electron beam energy axis along the $n = 2$ RR cut. As a result, a Lorentzian profile, the convergence of a Fano profile, was used in the present analysis.

To take account of the energy spread of the electron beam which is usually described with a Gaussian profile, the combined profile, therefore, is the convolution of a Gaussian and a Lorentzian profile, i.e., a Voigt profile. The normalized Voigt profile $V(E)$ can be expressed as

$$V(E) = \frac{2\ln 2}{\pi^{3/2}}\frac{\Gamma}{\omega^2} \times \int_{-\infty}^{\infty} \frac{\exp(-t^2)}{(\sqrt{\ln 2}\Gamma/\omega)^2 + [\sqrt{4\ln 2}(E - E_{\rm res})/\omega - t]^2} dt, \tag{7}$$

where ω is energy spread of the electron beam. The natural width Γ and the angular correction coefficient W were also calculated using FAC and listed in Tables I to VI. All of the natural widths were calculated with the Breit interaction, and listed following the corresponding doubly excited states. In addition, the $n = 2$ RR cross sections were also calculated within the interested electron energy range which is from 44 to 52 keV.

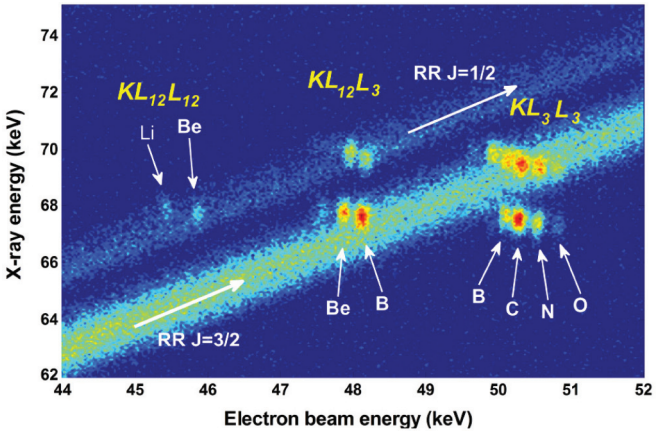

FIG. 2. (Color online) Two-dimensional scatter plot of x-ray intensity as functions of x-ray and electron energies.

TABLE I. Calculated Li-like gold KLL DR resonance energies $E_{\rm res}$ (keV), x-ray energies E_{hv} (keV), angular distribution correction coefficients W, resonance strengths S (10^{-20} cm^2 eV) (C + B = Coulomb + Breit, C = Coulomb only), and natural line widths Γ (eV). $|d\rangle$ and $|f\rangle$ stand for the doubly excited and final states, respectively.

$\|d\rangle$	$\|f\rangle$	$E_{\rm res}$	E_{hv}	W	$S^{\rm C+B}$	$S^{\rm C}$	Γ
$[1s2s^22p_{1/2}]_1$	$[2s^2]_0$	45.426	67.937	1.04	2.735	1.296	10.3
$[(1s2s)_12p_{1/2}^2]_1$	$[2s2p_{1/2}]_0$	45.580	67.899	0.99	0.089	0.089	14.2
	$[2s2p_{1/2}]_1$		67.864	1.00	0.170	0.171	
$[(1s2s)_02p_{1/2}^2]_0$	$[2s2p_{1/2}]_1$	45.759	68.042	1.00	0.090	0.088	16.9
$[1s2s^22p_{3/2}]_2$	$[2p_{1/2}2p_{3/2}]_1$	47.495	67.517	1.18	0.407	0.370	0.8
	$[2p_{1/2}2p_{3/2}]_2$		67.499	0.82	0.404	0.367	
$[1s2s^22p_{3/2}]_1$	$[2s^2]_0$	47.549	70.059	1.06	0.287	0.264	22.4
$[((1s2s)_12p_{1/2})_{1/2}2p_{3/2}]_2$	$[2s2p_{3/2}]_2$	47.565	67.883	0.76	0.134	0.068	6.0
$[((1s2s)_12p_{1/2})_{3/2}2p_{3/2}]_3$	$[2s2p_{3/2}]_2$	47.578	67.896	1.17	1.860	1.950	9.6
$[((1s2s)_12p_{1/2})_{1/2}2p_{3/2}]_1$	$[2s2p_{1/2}]_0$	47.648	69.967	1.02	0.063	0.061	27.9
$[((1s2s)_12p_{1/2})_{3/2}2p_{3/2}]_2$	$[2s2p_{1/2}]_1$	47.675	69.958	1.13	0.984	1.127	21.4
	$[2s2p_{3/2}]_2$		67.993	0.87	0.122	0.140	
	$[2s2p_{3/2}]_1$		67.895	1.13	0.416	0.477	
$[((1s2s)_12p_{1/2})_{3/2}2p_{3/2}]_1$	$[2s2p_{1/2}]_0$	47.723	70.042	1.26	0.292	0.313	28.2
	$[2s2p_{1/2}]_1$		70.007	0.87	0.329	0.352	
	$[2s2p_{3/2}]_1$		67.943	0.87	0.256	0.274	
$[((1s2s)_02p_{1/2})_{1/2}2p_{3/2}]_2$	$[2s2p_{1/2}]_1$	47.821	70.104	1.24	0.649	0.813	14.9
	$[2s2p_{3/2}]_2$		68.139	0.76	0.273	0.340	
	$[2s2p_{3/2}]_1$		68.041	1.24	0.358	0.448	
$[((1s2s)_02p_{1/2})_{1/2}2p_{3/2}]_1$	$[2s2p_{1/2}]_1$	47.824	70.107	0.89	0.011	0.071	7.5
$[(1s2s)_1(2p_{3/2}^2)_2]_3$	$[2s2p_{3/2}]_2$	49.640	69.959	1.17	1.164	0.923	5.9
$[(1s2s)_1(2p_{3/2}^2)_2]_2$	$[2s2p_{3/2}]_2$	49.749	70.067	0.87	0.337	0.531	26.4
$[(1s2s)_1(2p_{3/2}^2)_0]_1$	$[2s2p_{3/2}]_2$	49.789	70.108	1.00	0.279	0.178	16.5
$[(1s2s)_1(2p_{3/2}^2)_2]_1$	$[2s2p_{3/2}]_1$	49.829	70.050	0.88	0.103	0.238	32.6
$[(1s2s)_0(2p_{3/2}^2)_2]_2$	$[2s2p_{3/2}]_2$	49.896	70.215	0.77	0.202	0.184	11.3
	$[2s2p_{3/2}]_1$		70.117	1.23	0.443	0.404	
$[(1s2s)_0(2p_{3/2}^2)_0]_0$	$[2s2p_{3/2}]_1$	49.965	70.185	1.00	0.115	0.072	15.9

IV. RESULTS AND ANALYSIS

The experimental x-ray spectrum was obtained by projecting the x-ray counts onto the electron beam energy axis along the $n = 2$ RR cut, including both the $J = \frac{1}{2}$ and $J = \frac{3}{2}$ bands, as shown in Fig. 3. The gray dots with statistical errors are the experimental results. The statistical errors are between 3% and 6%. The x-ray spectrum consists of RR and DR events, the peaks are the DR events of Li-like to O-like gold ions, whereas the continuous background is from $n = 2$ RR. Corresponding

TABLE II. Same as Table I, but for Be-like gold.

$\|d\rangle$	$\|f\rangle$	$E_{\rm res}$	E_{hv}	W	$S^{\rm C+B}$	$S^{\rm C}$	Γ
$[1s2s^22p_{1/2}^2]_{1/2}$	$2p_{1/2}$	45.863	67.782	1.00	0.673	0.603	15.2
$[(1s2s^22p_{1/2})_12p_{3/2}]_{5/2}$	$2p_{3/2}$	47.864	67.804	1.20	2.964	3.167	10.3
$[(1s2s^22p_{1/2})_12p_{3/2}]_{3/2}$	$2p_{1/2}$	47.867	69.786	1.25	0.147	0.044	11.3
	$2p_{3/2}$		67.807	0.80	0.322	0.096	
$[(1s2s^22p_{1/2})_12p_{3/2}]_{1/2}$	$2p_{1/2}$	47.899	69.819	1.00	0.082	0.013	31.8
$[(1s2s^22p_{1/2})_02p_{3/2}]_{3/2}$	$2p_{1/2}$	47.949	69.869	1.25	1.690	2.555	20.7
	$2p_{3/2}$		67.889	0.80	0.228	0.345	
$[1s2s^2(2p_{3/2})_2^2]_{5/2}$	$2p_{3/2}$	49.914	69.854	1.20	1.684	1.353	6.2
$[1s2s^2(2p_{3/2})_2^2]_{3/2}$	$2p_{3/2}$	49.981	69.921	0.80	0.349	0.794	32.5
$[1s2s^2(2p_{3/2})_0^2]_{1/2}$	$2p_{3/2}$	50.012	69.952	1.00	0.470	0.301	16.7

TABLE III. Same as Table II, but for B-like gold.

$\|d\rangle$	$\|f\rangle$	$E_{\rm res}$	$E_{h\nu}$	W	$S^{\rm C+B}$	$S^{\rm C}$	Γ
$[1s2s^22p_{1/2}^22p_{3/2}]_2$	$(2p_{1/2}2p_{3/2})_1$	48.099	67.657	1.21	0.759	0.831	15.1
	$(2p_{1/2}2p_{3/2})_2$		67.639	0.79	0.745	0.815	
$[1s2s^22p_{1/2}^22p_{3/2}]_1$	$(2p_{1/2}^2)_0$	48.152	69.629	1.20	0.730	0.862	36.4
	$(2p_{1/2}2p_{3/2})_1$		67.710	0.90	0.090	0.106	
	$(2p_{1/2}2p_{3/2})_2$		67.692	1.02	0.427	0.504	
$[(1s2s^22p_{1/2})_1(2p_{3/2})_2^2]_2$	$(2p_{1/2}2p_{3/2})_1$	50.088	69.646	1.18	0.106	0.090	15.8
	$(2p_{1/2}2p_{3/2})_2$		69.628	0.82	0.274	0.233	
	$(2p_{3/2})_2^2$		67.681	0.82	0.313	0.266	
$[(1s2s^22p_{1/2})_1(2p_{3/2})_2^2]_3$	$(2p_{1/2}2p_{3/2})_2$	50.089	69.629	1.17	0.356	0.284	15.8
	$(2p_{3/2})_2^2$		67.682	1.17	0.631	0.502	
$[(1s2s^22p_{1/2})_1(2p_{3/2})_2^2]_1$	$(2p_{1/2}2p_{3/2})_1$	50.132	69.690	0.88	0.082	0.185	41.9
$[(1s2s^22p_{1/2})_1(2p_{3/2})_0^2]_1$	$(2p_{1/2}2p_{3/2})_2$	50.176	69.716	1.00	0.177	0.113	26.2
	$(2p_{3/2})_0^2$		67.699	1.00	0.129	0.082	
$[(1s2s^22p_{1/2})_0(2p_{3/2})_2^2]_2$	$(2p_{1/2}2p_{3/2})_1$	50.186	69.744	1.24	0.048	0.088	31.8
	$(2p_{1/2}2p_{3/2})_2$		69.726	0.76	0.193	0.353	
$[(1s2s^22p_{1/2})_0(2p_{3/2})_0^2]_0$	$(2p_{1/2}2p_{3/2})_1$	50.229	69.787	1.00	0.114	0.072	16.2

TABLE IV. Same as Table III, but for C-like gold.

$\|d\rangle$	$\|f\rangle$	$E_{\rm res}$	$E_{h\nu}$	W	$S^{\rm C+B}$	$S^{\rm C}$	Γ
$[1s2s^22p_{1/2}^2(2p_{3/2}^2)_2]_{5/2}$	$[2p_{1/2}^22p_{3/2}]_{3/2}$	50.272	69.428	1.20	0.454	0.361	20.4
	$[2p_{1/2}(2p_{3/2})_2^2]_{3/2}$		67.538	1.20	0.654	0.519	
	$[2p_{1/2}(2p_{3/2})_2^2]_{5/2}$		67.515	0.77	0.554	0.440	
$[1s2s^22p_{1/2}^2(2p_{3/2}^2)_2]_{3/2}$	$(2p_{1/2}^22p_{3/2})_{3/2}$	50.337	69.494	0.80	0.223	0.503	46.4
	$[2p_{1/2}(2p_{3/2})_2^2]_{5/2}$		67.581	1.05	0.085	0.192	
$[1s2s^22p_{1/2}^2(2p_{3/2}^2)_0]_{1/2}$	$[2p_{1/2}^22p_{3/2}]_{3/2}$	50.367	69.523	1.00	0.225	0.142	30.8
	$[2p_{1/2}(2p_{3/2})_0^2]_{1/2}$		67.551	1.00	0.209	0.132	

TABLE V. Same as Table IV, but for N-like gold.

$\|d\rangle$	$\|f\rangle$	$E_{\rm res}$	$E_{h\nu}$	W	$S^{\rm C+B}$	$S^{\rm C}$	Γ
$[1s2s^22p_{1/2}^2(2p_{3/2}^3)_{3/2}]_2$	$[2p_{1/2}^2(2p_{3/2})_2^2]_2$	50.535	69.330	1.10	0.457	0.380	30.8
	$[2p_{1/2}(2p_{3/2})_{3/2}^3]_1$		67.430	0.90	0.212	0.176	
	$[2p_{1/2}(2p_{3/2})_{3/2}^3]_2$		67.411	1.10	0.205	0.170	
$[1s2s^22p_{1/2}^2(2p_{3/2}^3)_{3/2}]_1$	$[2p_{1/2}^2(2p_{3/2})_2^2]_2$	50.586	69.381	0.98	0.152	0.200	50.9
	$[2p_{1/2}^2(2p_{3/2})_0^2]_0$		69.313	0.75	0.062	0.081	
	$[2p_{1/2}(2p_{3/2})_{3/2}^3]_2$		67.462	0.98	0.074	0.097	

TABLE VI. Same as Table V, but for O-like gold.

$\|d\rangle$	$\|f\rangle$	$E_{\rm res}$	$E_{h\nu}$	W	$S^{\rm C+B}$	$S^{\rm C}$	Γ
$[1s2s^22p_{1/2}^2(2p_{3/2}^4)]_{1/2}$	$[2p_{1/2}^2(2p_{3/2})_{3/2}^3]_{3/2}$	50.808	69.210	1.00	0.252	0.258	45.7
	$[2p_{1/2}(2p_{3/2})^4]_{1/2}$		67.325	1.00	0.119	0.122	

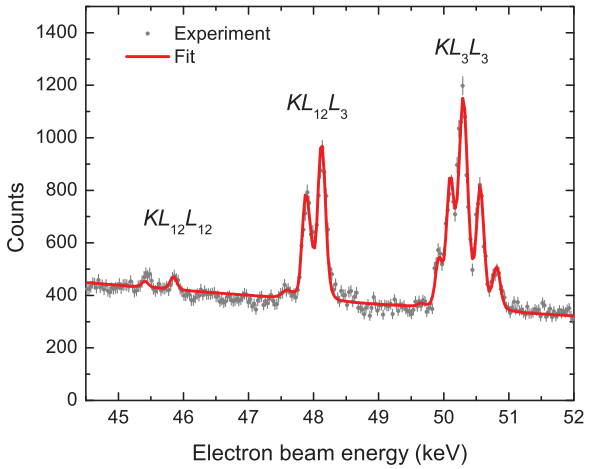

FIG. 3. (Color online) Experimental excitation function of *KLL* DR (gray dots) and the theoretical resonance function fitted to the experimental data (red curve).

to Fig. 2, the three peak groups are $KL_{12}L_{12}$, $KL_{12}L_3$, and KL_3L_3 DR resonances, respectively. The DR peaks can be distinguished clearly although overlapping exists. The smaller quantity of counts for Li-like and Be-like DR events in the $KL_{12}L_{12}$ region is attributed to the smaller fraction of these ions. The following expression was used to fit the experimental excitation function of Li-like to O-like gold ions:

$$F(E) = C(E)\sum_q f_q \left[\frac{d\sigma_{\rm RR}(q,E)}{d\Omega} + K_q \sum_{i,d,f} \frac{dS_{idf}}{d\Omega} V(E)\right], \tag{8}$$

where $C(E)$ is the detecting efficiency, f_q the ion abundance for the charge state q, $d\sigma_{\rm RR}(q,E)/d\Omega$ the differential cross section of $n = 2$ RR at 90°, K_q the independent amplitude factor used for correcting theoretical resonance strengths, and $V(E)$ the Voigt profile as shown in Eq. (7). The fitted parameters are the detection efficiency coefficient $C(E)$, the ion abundance f_q, the resonant strength correction factor K_q, and Gaussian width ω of the electron beam energy

A two-step process is used in the present analysis, which is similar to that used by Knapp [19] and Yao [37]. In the primary fitting, $C(E)$, f_q, and ω are free parameters, but K_q is fixed as $K_q = 1$. Using the theoretical DR resonance strengths including the Breit interaction effect, we obtained the detection efficiency coefficient $C(E)$, Gaussian width ω of the electron energy, and the ion abundance f_q. For the final fitting, we fixed $C(E)$, f_q, and ω obtained in the primary fitting, leaving K_q as a free parameter. In this analysis, experimental resonance strengths were obtained by multiplying the theoretic resonance strength by K_q. The fitting procedures were all weighted by the statistical uncertainties of the experimental data.

The final fitting result is shown as Fig. 3, and the fitted ion abundance f_q is listed in Table VII. In Fig. 3, the red solid line is the fitting result, which contains the contribution of RR and all of the DR resonances. Figure 3 shows a good agreement between the fitting and the experiment.

The total experimental resonance strengths obtained using Eq. (3) are listed in Table VIII, as well as the corresponding theoretical results. The uncertainties of experimental values

TABLE VII. The ion abundance f_q (%) obtained from the fitting.

Parameter						
	Li	Be	B	C	N	O
f_q	0.4	4.9	15.3	24.8	27.5	27.1

are listed in parentheses. Apart from the statistical errors and the fitting errors estimated in the fitting procedure, there are another two contributions impacting the total uncertainties. The first contribution is the accuracy of the RR cross-section calculation, which gives an uncertainty about 3%. The other one is from using the theoretical resonant strengths in the primary fit. Following the discussion in Ref. [37], we took 3% for this uncertainty estimation. The comparison in Table VIII shows that the experimental results agree well with the theoretical calculations within the error bars for Li-like to O-like ions. The present calculations show that the Breit interaction gives a strong enhancement for some specific resonance strengths and it is not so significant for the total resonance strengths. It is noted that there is large uncertainty for the Li-like ion. The smaller fraction is the main contribution to the uncertainty of the resonance strength of the Li-like ion.

In the work by Watanabe *et al.* [22], the total resonance strengths of He-like ions were fitted with equation

$$S = \frac{1}{m_1 Z^2 + m_2 Z^{-2}}, \tag{9}$$

where m_1 and m_2 are the free fit parameters and Z is the atomic number. This scaling formula was later extended to Li-like and Be-like ions [24]. Following the instruction in Ref. [24], this scaling formula is applicable for the other isoelectronic sequences (Li- to O-like ions) in this study. Figure 4 shows the plots of the scaling functions for the KLL DR resonances of Li- to O-like ions. The experimental results for Li-like ions are Fe^{23+}, Y^{36+}, Ho^{64+}, and Bi^{80+} by Kavanagh *et al.* [24], Kr^{33+} by Hu *et al.* [42], I^{50+} by Watanabe *et al.* [25] and Kavanagh *et al.* [24], Xe^{51+} by Yao *et al.* [37], and Au^{76+} obtained in this work. The theoretical results are from the same work as in the experiment, but Kr^{33+} by Fuchs *et al.* [20], I^{50+} by Kavanagh *et al.* [24] and Shi *et al.* [43].

Figure 4(a) shows the comparison between the present result of Li-like gold and the existing experimental results of Li-like ions. The results in Fig. 4(b) are taken from the same works as in Fig. 4(a), but for Be-like ions. The results of B-like and C-like ions are also taken from the same references as plotted in Figs. 4(c) and 4(d).

TABLE VIII. Experimental and theoretical resonance strengths (C + B = Coulomb + Breit, C = Coulomb only) for KLL DR resonance of highly charged gold (in units of 10^{-20} cm^{2}eV).

Ions	Experiment	Theory C + B	Theory C
Li-like	16.72(9.40)	12.96	12.01
Be-like	8.98(1.04)	8.84	9.45
B-like	5.43(0.44)	5.29	5.57
C-like	2.48(0.21)	2.43	2.34
N-like	1.27(0.15)	1.18	1.12
O-like	0.48(0.11)	0.37	0.38

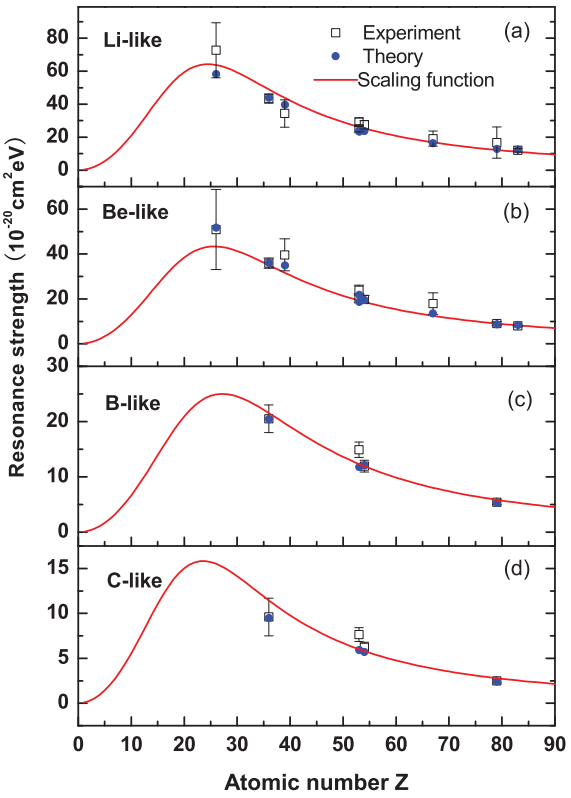

FIG. 4. (Color online) Resonance strengths of the KLL resonance of Li- to C-like ions against atomic number. The experimental results for Li-like ions are Fe^{23+}, Y^{36+}, Ho^{64+}, and Bi^{80+} by Kavanagh *et al.* [24], Kr^{33+} by Hu *et al.* [42], I^{50+} by Watanabe *et al.* [25] and Kavanagh *et al.* [24], Xe^{51+} by Yao *et al.* [37], and Au^{76+} obtained in this work. The theoretical results are taken from the same work as the experiment, but Kr^{33+} by Fuchs *et al.* [20], I^{50+} by Kavanagh *et al.* [24] and Shi *et al.* [43]. For Li- and Be-like ions, the values of m_1 and m_2 of the scaling functions [Eq. (9)] are taken from Ref. [24]. The results of Be-like to C-like ions are also taken from the same references. For B- and C-like ions, the values of m_1 and m_2 are obtained by fitting the existing and present data points.

The values of m_1 and m_2 for Li-like and Be-like ions are taken from Ref. [24]. As shown in Figs. 4(a) and 4(b), the present results of Li-like and Be-like ions agree well with the existing scaling functions. For B-like and C-like ions, the values are determined by weighted least-squares fitting of the scaling formula described by Eq. (9). The presently obtained parameters m_1 and m_2 are listed in Table IX. Since fewer measurements are available for the B-like and C-like ions, the present m_1 and m_2 have relatively large errors; this is in particular true for m_2, which is determined predominantly by the experimental results of lower-Z ions. The lack of DR resonance strength measurements for lower-Z ions increased the fitting uncertainties. In the future, more experimental measurements with higher precision, especially in the lower-Z region, are required to determine the values of m_1 and m_2 in the scaling formula.

TABLE IX. Parameters m_1 and m_2 obtained by fitting the function $\frac{1}{m_1 Z^2 + m_2 Z^{-2}}$ to various sets of measurements of KLL dielectronic recombination of B-like and C-like ions.

Ions	$m_1(10^{15}$ cm^{-2} eV$^{-1})$	$m_2(10^{20}$ cm^{-2} eV$^{-1})$
B-like	2.70 ± 0.17	14.80 ± 8.14
C-like	5.70 ± 0.38	17.51 ± 22.83

V. CONCLUSIONS

KLL DR of Li- to O-like gold ions has been measured with the Tokyo-EBIT. The experimental resonance strengths have been obtained by normalizing the DR x-ray counts to the theoretical RR cross sections. The theoretical DR resonance strengths and the RR cross sections were calculated using the flexible atomic code. The present experimental results agree well with the theoretical calculations within the uncertainties, and reaffirm the accuracy of FAC calculations for high-Z ions although it has been demonstrated at low-Z ions by Bitter *et al.* [38]. KLL DR resonance strengths of Li-like and Be-like gold agree well with the existing scaling functions. In addition, the scaling laws of the KLL DR resonance strengths were obtained as a function of atomic number for B-like and C-like ions by fitting the present and existing experimental results.

ACKNOWLEDGMENTS

This work is supported by the Foundation of Science and Technology on Plasma Physics Laboratory (Grant No. 9140C6804010906) and the Science and Technology Foundation of China Academy of Engineering Physics (Grant No. 2013A0102002). The authors would like to thank Dr. H. Watanabe for his helpful discussions.

[1] M. E. Foord, S. H. Glenzer, R. S. Thoe, K. L. Wong, K. B. Fournier, B. G. Wilson, and P. T. Springer, Phys. Rev. Lett. **85**, 992 (2000).

[2] K. L. Wong, M. J. May, P. Beiersdorfer, K. B. Fournier, B. Wilson, G. V. Brown, P. Springer, P. A. Neill, and C. L. Harris, Phys. Rev. Lett. **90**, 235001 (2003).

[3] M. J. May, S. B. Hansen, J. Scofield, M. Schneider, K. Wong, and P. Beiersdorfer, Phys. Rev. E **84**, 046402 (2011).

[4] P. Beiersdorfer, M. J. May, J. H. Scofield, and S. B. Hansen, High Energy Density Phys. **8**, 271 (2012).

[5] N. Nakamura, A. P. Kavanagh, H. Watanabe, H. A. Sakaue, Y. M. Li, D. Kato, F. J. Currell, and S. Ohtani, Phys. Rev. Lett. **100**, 073203 (2008).

[6] D. Bernhardt *et al.*, Phys. Rev. A **83**, 020701(R) (2011).

[7] D. A. Knapp, P. Beiersdorfer, M. H. Chen, J. H. Scofield, and D. Schneider, Phys. Rev. Lett. **74**, 54 (1995).

[8] A. J. González Martínez, J. R. Crespo López-Urrutia, J. Braun, G. Brenner, H. Bruhns, A. Lapierre, V. Mironov, R. Soria Orts, H. Tawara, M. Trinczek, J. Ullrich, and J. H. Scofield, Phys. Rev. Lett. **94**, 203201 (2005).

[9] H. Watanabe, A. P. Kavanagh, H. Kuramoto, Y. M. Li, N. Nakamura, S. Ohtani, B. O'Rourke, A. Sato, H. Tawara, X. Tong, and F. J. Currell, Nucl. Instrum. Methods Phys. Res., Sect. B **235**, 261 (2005).
[10] B. E. O'Rourke, F. J. Currell, H. Kuramoto, S. Ohtani, H. Watanabe, Y. M. Li, T. Tawara, and X. M. Tong, Phys. Rev. A **77**, 062709 (2008).
[11] D. R. DeWitt, D. Schneider, M. W. Clark, M. H. Chen, and D. Church, Phys. Rev. A **44**, 7185 (1991).
[12] D. R. DeWitt, R. Schuch, T. Quinteros, H. Gao, W. Zong, H. Danared, M. Pajek, and N. R. Badnell, Phys. Rev. A **50**, 1257 (1994).
[13] Z. Hu, Y. Li, and N. Nakamura, Phys. Rev. A **87**, 052706 (2013).
[14] Z. Hu, Y. Li, A. Yamazaki, and N. Nakamura, Phys. Scr., T **144**, 014047 (2011).
[15] A. J. Smith, P. Beiersdorfer, K. Widmann, M. H. Chen, and J. H. Schofield, Phys. Rev. A **62**, 052717 (2000).
[16] R. Ali, C. P. Bhalla, C. L. Cocke, and M. Stockli, Phys. Rev. Lett. **64**, 633 (1990).
[17] P. Beiersdorfer, T. W. Phillips, K. L. Wong, R. E. Marrs, and D. A. Vogel, Phys. Rev. A **46**, 3812 (1992).
[18] D. A. Knapp, R. E. Marrs, M. A. Levine, C. L. Bennett, M. H. Chen, J. R. Henderson, M. B. Schneider, and J. H. Scofield, Phys. Rev. Lett. **62**, 2104 (1989).
[19] D. A. Knapp, R. E. Marrs, M. B. Schneider, M. H. Chen, M. A. Levine, and P. Lee, Phys. Rev. A **47**, 2039 (1993).
[20] T. Fuchs, C. Biedermann, R. Radtke, E. Behar, and R. Doron, Phys. Rev. A **58**, 4518 (1998).
[21] Y. Zou, J. R. Crespo López-Urrutia, and J. Ullrich, Phys. Rev. A **67**, 042703 (2003).
[22] H. Watanabe, F. J. Currell, H. Kuramoto, Y. M. Li, S. Ohtani, B. O'Rourke, and X. M. Tong, J. Phys. B: At., Mol. Opt. Phys. **34**, 5095 (2001).
[23] B. E. O'Rourke, H. Kuramoto, Y. M. Li, S. Ohtani, X. M. Tong, H. Watanabe, and F. J. Currell, J. Phys. B: At., Mol. Opt. Phys. **37**, 2343 (2004).
[24] A. P. Kavanagh, H. Watanabe, Y. M. Li, B. E. O'Rourke, H. Tobiyama, N. Nakamura, S. McMahon, C. Yamada, S. Ohtani, and F. J. Currell, Phys. Rev. A **81**, 022712 (2010).
[25] H. Watanabe, H. Tobiyama, A. P. Kavanagh, Y. M. Li, N. Nakamura, H. A. Sakaue, F. J. Currell, and S. Ohtani, Phys. Rev. A **75**, 012702 (2007).
[26] M. B. Schneider, D. A. Knapp, M. H. Chen, J. H. Scofield, P. Beiersdorfer, C. L. Bennett, J. R. Henderson, R. E. Marrs, and M. A. Levine, Phys. Rev. A **45**, R1291 (1992).
[27] M. J. May, K. B. Fournier, P. Beiersdorfer, H. Chen, and K. L. Wong, Phys. Rev. E **68**, 036402 (2003).
[28] M. B. Schneider, R. Mancini, K. Widmann, K. B. Fournier, G. V. Brown, H. K. Chung, H. A. Baldis, S. B. Cone, K. Hansen, M. J. May, D. Thorn, and P. Beiersdorfer, Can. J. Phys. **86**, 259 (2008).
[29] M. F. Gu, Astrophys. J. **582**, 1241 (2003).
[30] M. F. Gu, Can. J. Phys. **86**, 675 (2008).
[31] F. J. Currell, J. Asada, K. Ishii, M. Arimichi, K. Motohashi, N. Nakamura, K. Nishizawa, S. Ohtani, K. Okazaki, M. Sakurai, H. Shiraishi, S. Tsurubuchi, and H. Watanabe, J. Phys. Soc. Jpn. **65**, 3186 (1996).
[32] N. Nakamura, J. Asada, F. J. Currell, T. Fukami, T. Hirayama, K. Motohashi, T. Nagata, E. Nojikawa, S. Ohtani, K. Okazaki, M. Sakurai, H. Shiraishi, S. Tsurubuchi, and H. Watanabe, Phys. Scr., T **73**, 362 (1997).
[33] C. Yamada, K. Nagata, N. Nakamura, S. Ohtani, S. Takahashi, T. Tobiyama, M. Tona, H. Watanabe, N. Yoshiyasu, M. Sakurai, A. P. Kavanagh, and F. J. Currell, Rev. Sci. Instrum. **77**, 066110 (2006).
[34] Y. B. Fu, C. Z. Dong, M. G. Su, F. Koike, G. O'Sullivan, and J. G. Wang, Phys. Rev. A **83**, 062708 (2011).
[35] B. W. Li, G. O'Sullivan, Y. B. Fu, and C. Z. Dong, Phys. Rev. A **85**, 012712 (2012).
[36] U. I. Safronova and A. S. Safronova, Phys. Rev. A **85**, 032507 (2012).
[37] K. Yao, Z. Geng, J. Xiao, Y. Yang, C. Chen, Y. Fu, D. Lu, R. Hutton, and Y. Zou, Phys. Rev. A **81**, 022714 (2010).
[38] M. Bitter, M. F. Gu, L. A. Vainshtein, P. Beiersdorfer, G. Bertschinger, O. Marchuk, R. Bell, B. LeBlanc, K. W. Hill, D. Johnson, and L. Roquemore, Phys. Rev. Lett. **91**, 265001 (2003).
[39] M. F. Gu, P. Beiersdorfer, G. Brown, A. Graf, R. L. Kelley, C. Kilbourne, F. Porter, and S. Kahn, Can. J. Phys. **90**, 351 (2012).
[40] Z. Hu, X. Han, Y. Li, D. Kato, X. Tong, and N. Nakamura, Phys. Rev. Lett. **108**, 073002 (2012).
[41] N. Nakamura, A. P. Kavanagh, H. Watanabe, H. A. Sakaue, Y. Li, D. Kato, F. J. Currell, X.-M. Tong, T. Watanabe, and S. Ohtani, Phys. Rev. A **80**, 014503 (2009).
[42] Z. Hu, J. Yang, J. Zhang, T. Zhu, B. Zhang, Y. Ding, Z. Zheng, B. Duan, Y. Li, and J. Yan, Chin. Phys. Lett. **26**, 33401 (2009).
[43] Y. Shi, C. Dong, and D. Zhang, Phys. Lett. A **372**, 4913 (2008).